Surface Atomic Structure of KDP Crystals in Aqueous Solution: An Explanation of the Growth Shape

S. A. de Vries,[1] P. Goedtkindt,[1,2] S. L. Bennett,[3] W. J. Huisman,[1] M. J. Zwanenburg,[1] D.-M. Smilgies,[4]
J. J. De Yoreo,[5] W. J. P. van Enckevort,[6] P. Bennema,[6] and E. Vlieg[1]

[1]FOM-Institute for Atomic and Molecular Physics, Kruislaan 407, 1098 SJ Amsterdam, The Netherlands
[2]Universitaire Instelling Antwerpen, Department of Chemistry, Universiteitsplein 1, B-2610 Wilrijk, Belgium
[3]CCLRC, Daresbury Laboratory, Warrington WA4 4AD, United Kingdom
[4]European Synchrotron Radiation Facility, B.P. 220, 38043 Grenoble Cedex, France
[5]Lawrence Livermore National Laboratory, 7000 East Avenue, Livermore, California 94550
[6]RIM, Department of Solid State Chemistry, University of Nijmegen, Toernooiveld 1, 6525 ED Nijmegen, The Netherlands

With this study on KDP, we present an interface atomic structure determination of a crystal in contact with its growth solution. Using x-ray diffraction at a third-generation synchrotron radiation source, the structure of both the {101} and {100} faces has been determined. We found that the {101} faces are terminated by a layer of K^+ ions and not by $H_2PO_4^-$ groups, resolving a long-standing issue that could not be predicted by theory. This result leads to an atomic-scale explanation of the influence of metal impurities on the macroscopic growth morphology. [S0031-9007(98)05505-7]

The crystallographic theory of Hartman and Perdok aims to predict the morphology of growing crystals [1,2]. With this theory it is often possible to predict from a known crystal structure the facets, referred to by the Miller indices $(h\,k\,\ell)$, that will dominate the crystal form. These faces are the so-called F (flat) faces. Since the growth of crystals takes place at the crystal-solution interface, one expects the atomic structure at this boundary to play a primary role in the composition, growth, and morphology of the crystal. Hardly any atomic-scale experimental data exist to verify this. Hartman-Perdok theory does not take into account possible relaxations or reconstructions at the crystal surface, nor the influence of the solution on the interface, but is still remarkably successful. A problem in the theory is, however, that often more than one surface termination is possible for a given orientation $(h\,k\,\ell)$ and that it is impossible to predict which of the alternatives will control the crystal growth.

With the appearance of third-generation synchrotron radiation sources it is now possible to look accurately at the atomic structure of these interfaces with x rays. Surface x-ray diffraction has proven to be a very powerful technique for studying interfaces at an atomic scale [3], and it is one of the few surface science techniques that does not require a vacuum environment. X-ray scattering studies have been done on liquid-liquid [4] and liquid-solid interfaces [5,6]. In particular, surfaces of electrodes in an electrolyte solution have received attention [7,8]. Recently the first *in situ* x-ray diffraction studies on crystals in their growth solution have been reported [9,10]. Here we report the determination of the atomic positions at such an interface.

The system we study is a KH_2PO_4 (KDP) crystal in its aqueous growth solution. KDP finds widespread use as a frequency doubler in laser applications and has been stud-

ied in great detail [11]. Hartman-Perdok theory predicts that the pyramidal faces {101} and the prismatic faces {100} of KDP are flat in solution [12,13]. This is in agreement with the observed habit of these crystals: they exist as a tetragonal prism consisting of four faces of the form {100} terminated by two opposing tetragonal pyramids consisting of {101} faces [see Fig. 1(a)]. For the prismatic {100} faces exactly one surface termination is predicted. For the pyramidal {101} faces, however, two alternative terminations are theoretically possible. One has the negative $H_2PO_4^-$ groups on the outside, and the other the positive K^+ ions [see Fig. 1(b)].

For these pyramidal faces the question arises whether growth kinetics is determined by single layers, with alternately K^+ and $H_2PO_4^-$ on top, or double layers. The single layers are strongly polar. The difference in polarity of the layers and, especially, the differences in size and polarizability of the ions will result in a different surface free energy. If the polarity of the surface layers does not play a role in the step kinetics, the surface would consist of both K^+ and $H_2PO_4^-$-terminated layers. From the surface morphology observed with interference-contrast reflection microscopy and considering the symmetry of the crystal [13,14] it can be concluded that the surface is bounded by only one of the polar layers. This is confirmed by atomic force microscopy measurements where the height of the steps on the {101} face is always found to correspond to the thickness of double layers [15].

The question remains which of the two alternative layers is the one at the surface. We have determined the surface structure of both the {101} and {100} surfaces in solution by measuring the distribution of diffracted intensities along so-called crystal truncation rods (CTRs) [16]. These CTRs are tails of diffuse intensity connecting the bulk Bragg
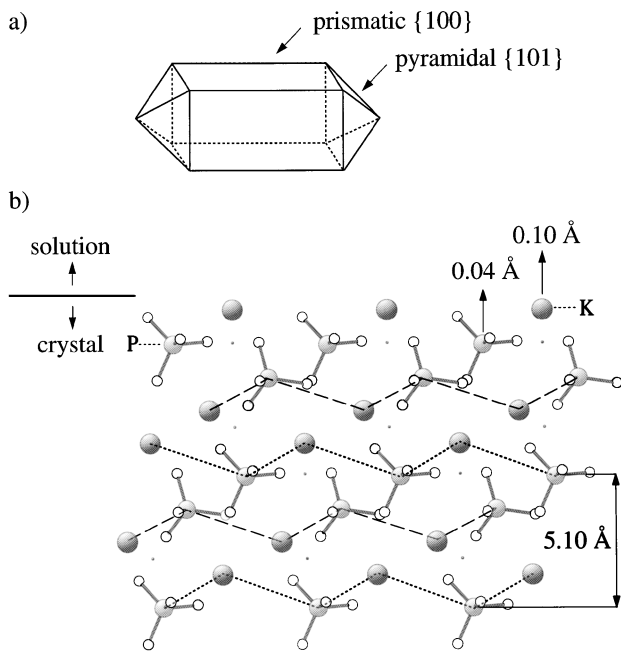
FIG. 1. (a) Growth habit of a KDP crystal with the prismatic and pyramidal faces indicated. (b) Schematic side view of the pyramidal face, KDP(101), projected on the (111) plane. The big circles are the potassium atoms while the PO_4 groups are depicted as a circle for the phosphor atom connected by sticks to the four neighboring oxygen atoms, shown as small white circles. The dots give the positions of the hydrogen atoms between two oxygen atoms. The layers with the K^+ ions on top are schematically indicated by the dotted lines and the layers with the $H_2PO_4^-$ groups on top by the dashed lines. Arrows indicate the relaxations in the topmost layer as determined from fitting the experimental data.

peaks in the direction perpendicular to the surface and show the interference between bulk and surface structure. Parallel to the interface the aqueous solution will be very weakly ordered [8]. We have only measured CTRs which have an in-plane component (i.e., not the specular rod), for which the intensity distribution will hardly be influenced by the solution and mainly depends on the crystal surface atomic structure.

For KDP(101) we use a unit cell of which the primitive lattice vectors $\{a_i\}$ can be expressed in the conventional tetragonal lattice vectors as $a_1 = \frac{1}{2}[1\,1\,1]_{\text{tetragonal}}$, $a_2 = \frac{1}{2}[\bar{1}\,1\,\bar{1}]_{\text{tetragonal}}$, and $a_3 = [\bar{1}\,0\,1]_{\text{tetragonal}}$, with $|a_1| = |a_2| = \sqrt{\frac{1}{2}a^2 + \frac{1}{4}c^2}$, $|a_3| = \sqrt{a^2 + c^2}$, with $a = 7.45$ Å and $c = 6.97$ Å the lattice constants of bulk KDP [17]. The corresponding reciprocal lattice vectors $\{b_i\}$ are defined by $a_i \cdot b_j = 2\pi\delta_{ij}$. The momentum transfer vector Q, which is the difference between the wave vectors of the incident and scattered x rays, can be denoted by the diffraction indices $(hk\ell)$ in reciprocal space: $Q = hb_1 + kb_2 + \ell b_3$. For CTRs, which are labeled by (hk), the indices h and k have integer values, whereas ℓ is unconstrained and refers to the component of Q perpendicular to the surface. The Bragg peaks occur for integer values of ℓ,

which is in reciprocal lattice units (r.l.u.) of 0.62 Å^{-1}. For KDP(100) we use a unit cell in which the primitive lattice vectors are $a_1 = [0\,1\,0]_{\text{tetragonal}}$, $a_2 = [0\,0\,1]_{\text{tetragonal}}$, and $a_3 = [1\,0\,0]_{\text{tetragonal}}$. These definitions result in 1 r.l.u. $= 0.84$ Å^{-1} along the ℓ direction.

The measurements were performed at the TROIKA open undulator beam line (ID10A) of the European Synchrotron Radiation Facility (ESRF) in Grenoble, France [18]. These data were fully consistent with earlier measurements (with a lower accuracy) performed at the Synchrotron Radiation Source in Daresbury, U.K. The crystals were mounted in a growth chamber made of polycarbonate, consisting of an outer heating bath kept at a constant temperature by a thermostat. In the inner chamber, the crystal is mounted in an environment of a saturated aqueous KDP solution. The structure determination was carried out at a temperature of 22 °C. The incoming and outgoing x-ray beams penetrate through a thin Mylar foil (6 μm) which can be pushed close to the crystal surface, leaving a thin layer of saturated solution between the crystal and the foil (thickness $\sim$ 10 μm). The crystal growth chamber is mounted onto a horizontal diffractometer (i.e., the scattering plane is horizontal). The beryllium monochromator was set to select a wavelength of 0.73 Å (17.0 keV) using the (002) reflection, leading to approximately 10^{12} photons/sec in a 2 × 1 mm^2 spot. This wavelength was chosen as an optimum in the signal to background ratio. For smaller wavelengths the diffuse background scattering from the bulk crystal rapidly goes up, while for larger wavelengths attenuation in the solution (and the Mylar) becomes too strong. For a typical surface reflection the signal-to-background ratio is about 10%, but for weak reflections this can be as small as 2%. The possibility to do accurate measurements under these circumstances has enormously increased with the availability of high-intensity and high-energy x-ray beams from third-generation synchrotron radiation sources such as the ESRF. The KDP crystals are sufficiently flat to measure the CTR intensity far from the Bragg peaks, where the surface sensitivity is highest.

Figure 2 shows measured structure factor amplitudes along the $(h\,k) = (1\,0)$ CTR for KDP(101). The integrated intensity at each point ℓ is determined by rotating the crystal about the surface normal and measuring the number of diffracted photons. The measured integrated intensities are corrected for the active sample area, the Lorentz factor, the polarization factor, the rod interception [19], and the absorption due to the different pathways of the outgoing beam through the liquid and the Mylar foil. Structure factor amplitudes are obtained by taking the square root of the corrected integrated intensity. The values for the negative ℓ part of the rod are obtained according to Friedel's rule by inverting the structure factor distribution along the positive $(hk) = (\bar{1}0)$ rod through the origin of reciprocal space.

The dotted curve in Fig. 2 gives the expected values for a bulk K^+-terminated surface and the dashed curve
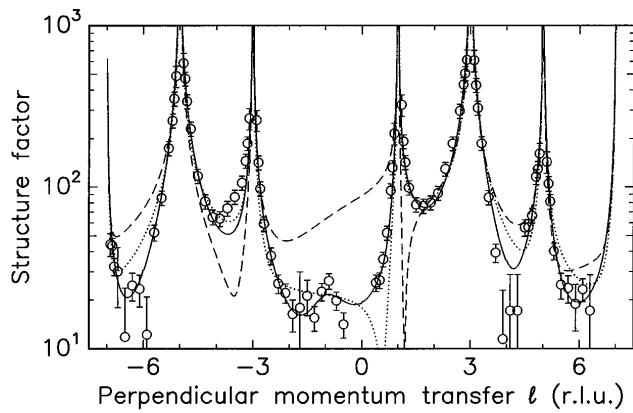
FIG. 2. Structure factor amplitudes along the $(hk) = (10)$ crystal truncation rod for KDP(101) as a function of the diffraction index ℓ which is expressed in reciprocal lattice units. The dotted line is a calculation for a bulk K^+-terminated surface, the dashed curve for a $H_2PO_4^-$-terminated one. The solid line is the best fit starting from a K^+-terminated surface and allowing the K^+ ions and the $H_2PO_4^-$ groups in the top layer to relax.

FIG. 3. Structure factor amplitudes along the $(hk) = (12)$ crystal truncation rod of KDP(100). The solid curve is a calculation for a bulk terminated crystal with a rms roughness of 1.2 Å.

is a calculation for a surface terminated by the $H_2PO_4^-$ groups. It is immediately clear that the surface must be K^+ terminated. Our data confirm the conclusion of De Yoreo, Land, and Dair [15] that the surface does not contain both K^+ and $H_2PO_4^-$-terminated parts. An even better description of the data is obtained when small out-of-plane relaxations of the top layer are allowed and when a simple model for surface roughness on an atomic scale is included [16]. Least-squares fitting of the data then results in a model that yields the solid line. A schematic side view of this model is shown in Fig. 1. The fit procedure was performed using the complete data set which also includes the $(h\,k) = (1\,1)$ and $(h\,k) = (2\,1)$ CTRs (not shown). In the best fit model the K atoms in the top layer relax outwards by an amount of 0.10 ± 0.05 Å and the H_2PO_4 groups by 0.04 ± 0.05 Å. The root mean square (rms) roughness was estimated to be 2.0 ± 0.5 Å measured over a lateral length scale of a few thousand Å.

In a similar fashion, data were obtained on KDP(100). In Fig. 3, structure factor amplitudes along the $(h\,k) = (1\,2)$ CTR are shown. For this surface only one bulk crystal termination is possible. The solid curve is a fit to the data using as fit parameters only a scale factor and a roughness parameter. For the fit the full data set was used that also contains parts of the $(h\,k) = (2\,1)$ and $(h\,k) = (3\,0)$ CTRs (not shown). The rms roughness found for this surface is 1.2 ± 0.3 Å. A schematic side view of the structure model is shown in Fig. 4. The data set on this face was much smaller than on KDP(101), and therefore we can only conclude that if there are relaxations of the top layer atoms these are smaller than 0.1 Å.

Having established the atomic structure of both faces, we can now understand why small traces of trivalent metal ion impurities like Fe^{3+} or Cr^{3+} block the growth of the prismatic faces, but affect the growth of the pyramidal faces to a much lesser extent [13,20,21]. When such impurities are present the crystals become more elongated in the direction of the pyramids. Looking at Figs. 1 and 4, it is seen that the pyramidal face has the K^+ ions on the outside of the crystal for the best fit model. The prismatic face has both the positive K^+ ions and the negative $H_2PO_4^-$ at the interface. This result supports the hypothesis of Dam *et al.* [13] that the attachment of cations to the pyramidal faces is less favorable than to the prismatic faces. With only K^+ ions on the surface of the crystal, metal impurities like Fe^{3+} and Cr^{3+} ions will experience a large barrier to adsorption onto the positively charged face. On the prismatic faces, however, these ions can adsorb easily, and small amounts of Fe^{3+} or Cr^{3+} will already block the growth.
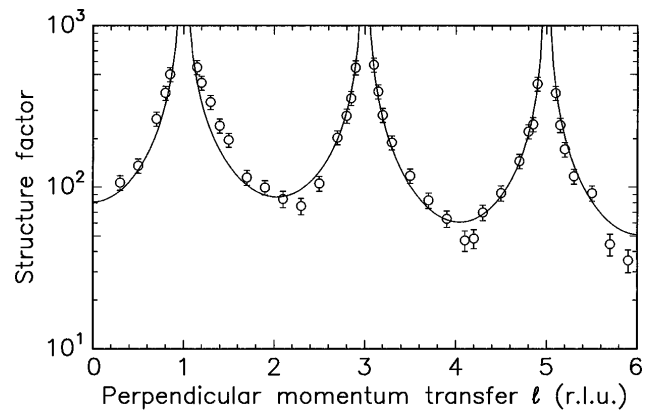
For the pyramidal growth sectors the segregation coefficient of trivalent metal ions has been found to be much lower than for the prismatic sectors [22]. Similar differences in impurity segregation on crystallographically dissimilar faces [23] as well as dissimilar steps on a single face [24] have been observed in other crystal systems grown from solutions. Paquette and Reader [24] attributed such inhomogeneities in $CaCO_3$ to differences in kink site
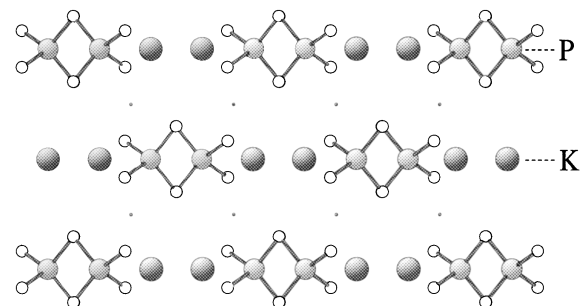
FIG. 4. The prismatic face KDP(100) projected on the (010) plane. Here only one termination is possible.

geometries, the implication being that incorporation kinetics at steps controlled the impurity content. We now have shown that for KDP a different mechanism is active, since the impurity content in the pyramidal sectors of the crystal is limited by adsorption kinetics on the terraces rather than incorporation kinetics at the steps.

Our results thus present an atomic-scale explanation for the influence of impurities on the macroscopic growth morphology of KDP. At the same time the possibility of determining the interface structure of a crystal in its growth solution is an important step towards the development of more sophisticated crystal growth theories. The atomic structure at the solid-liquid interface, including relaxations or even reconstructions, is important for controlling the distribution and concentration of the molecules in the solution. An intriguing implication of the present work is that a strongly polarized crystal surface will affect the structure of the near-surface liquid layer. Presumably there is a charge compensating layer of solution adjacent to the surface, and this must strongly affect the adsorption kinetics for the solute ions. In addition, the fact that the (101) surface is positively charged suggests that the reaction rate (desolvation and attachment) for anions is much greater than for cations. More experiments and theory are necessary to further increase our understanding of these phenomena.

[1] P. Hartman, in *Crystal Growth: An Introduction,* edited by P. Hartman (North-Holland, Amsterdam, 1973), Chap. 14, p. 367.

[2] P. Bennema, in *Handbook of Crystal Growth,* edited by D. T. J. Hurle (Elsevier Science Publishers, Amsterdam, 1993), Vol. 1a, Chap. 7, p. 477.

[3] R. Feidenhans'l, Surf. Sci. Rep. **10**, 105 (1989).

[4] B. R. McClain *et al.,* Phys. Rev. Lett. **72**, 246 (1994).

[5] B. M. Ocko, Phys. Rev. Lett. **64**, 2160 (1990).

[6] W. J. Huisman *et al.,* Nature (London) **390**, 379 (1997).

[7] B. M. Ocko, J. Wang, A. Davenport, and H. Isaacs, Phys. Rev. Lett. **65**, 1466 (1990).

[8] M. F. Toney *et al.,* Nature (London) **368**, 444 (1994).

[9] R. P. Chiarello and N. C. Sturchio, Geochim. Cosmochim. Acta **59**, 4557 (1995).

[10] D. Gidalevitz *et al.,* Angew. Chem. Int. Ed. Engl. **36**, 955 (1997).

[11] L. N. Rashkovich, *KDP-Family Single Crystals* (IOP Publishing Ltd., Bristol, 1991).

[12] P. Hartman, Acta Crystallogr. **9**, 721 (1956).

[13] B. Dam, P. Bennema, and W. J. P. van Enckevort, J. Cryst. Growth **74**, 118 (1986).

[14] W. J. P. van Enckevort, R. Janssen-van Rosmalen, and W. H. van der Linden, J. Cryst. Growth **49**, 502 (1980).

[15] J. J. De Yoreo, T. A. Land, and B. Dair, Phys. Rev. Lett. **73**, 838 (1994).

[16] I. K. Robinson, Phys. Rev. B **33**, 3830 (1986).

[17] R. J. Nelmes, Z. Tun, and W. F. Kuhs, Ferroelectrics **71**, 125 (1987).

[18] G. Grübel, J. Als-Nielsen, and A. K. Freund, J. Phys. IV (France) **4**, C9-27 (1994).

[19] E. Vlieg, J. Appl. Crystallogr. **30**, 532 (1997).

[20] B. Dam and W. J. P. van Enckevort, J. Cryst. Growth **69**, 306 (1984).

[21] B. Dam, E. Polman, and W. J. P. van Enckevort, in *Industrial Crystallization 84,* edited by S. J. Jančić and E. J. de Jong (Elsevier Science Publishers, Amsterdam, 1984), p. 97.

[22] C. Belouet, E. Dunia, and J. F. Pétroff, J. Cryst. Growth **23**, 243 (1974).

[23] Lu Taijing, R. B. Yallee, C. K. Ong, and I. Sunagawa, J. Cryst. Growth **151**, 342 (1995).

[24] J. Paquette and R. J. Reeder, Geochim. Cosmochim. Acta **59**, 735 (1995).